

Metal plasma immersion ion implantation and deposition: a review

André Anders

Lawrence Berkeley National Laboratory, University of California, Berkeley, CA 94720, USA

Abstract

Metal plasma immersion ion implantation and deposition (MePIIID) is a hybrid process combining cathodic arc deposition and plasma immersion ion implantation. The properties of a metal plasma produced by vacuum arcs are reviewed and the consequences for MePIIID are discussed. Different version of MePIIID are described and compared with traditional methods of surface modification such as ion beam assisted deposition (IBAD). MePIIID is a very versatile approach because of the wide range of ion species and energies used. At one extreme case, films are deposited with ions in the energy range 20–50 eV, and at the other extreme, ions can be implanted with high energy (100 keV or more) without film deposition. Novel features of the technique include the use of improved macroparticle filters; the implementation of several plasma sources for multi-element surface modification; tuning of ion energy during implantation and deposition to tailor the substrate-film intermixed layer and structure of the growing film; simultaneous pulsing of the plasma potential (positive) and substrate bias (negative) with a modified Marx generator; and the use of high ion charge states. © 1997 Elsevier Science S.A.

Keywords: Ion implantation and deposition; Metal plasma; Vacuum arc

1. Introduction

Plasma source ion implantation (PSII, also called plasma immersion ion implantation PIII or PI³, or plasma-based ion implantation, PBII) is a surface modification technique proposed and developed in the mid 1980s by Conrad and co-workers [1,2]. Much progress has been made in recent years [3–5], and the first commercial facilities have recently been built [6].

The basic idea works as follows: negative high voltage pulses are applied to a conductive substrate that is immersed in a gaseous plasma. During each pulse, an electric sheath forms adjacent to the substrate. Gas ions entering the sheath are accelerated towards and implanted into the substrate. PIII with gaseous plasmas (e.g. nitrogen, oxygen, BF₃, etc.) has become a well-established technique to modify surface properties, for instance for tribological [7,8] and semiconductor applications [5].

PIII with metal (and carbon) plasmas results in a qualitatively different kind of surface modification due to the condensable nature of the plasma. Generally, the technique includes both deposition and implantation phases: deposition of a film occurs in the time intervals between high voltage bias pulses and implantation occurs during the pulses.

In this paper, various versions of PIII using metal plasmas produced by vacuum arcs are reviewed. The term “metal plasmas” includes here also plasmas of semimetallic and semiconductor materials such as carbon, silicon and germanium. In Section 2, the plasma formation process and the properties of vacuum arc plasmas are described. In Section 3, various versions of the technique are discussed and novel approaches are presented. Some examples of film formation and ion implantation are given in Section 4. A new approach to PIII with metal plasmas is proposed in Section 5, and conclusions are drawn in Section 6.

2. Generation, properties and filtering of vacuum arc metal plasmas

A vacuum arc metal plasma is obtained when an arc discharge is initiated between two metal electrodes in vacuum. The plasma necessary for the current transport between the electrodes is formed at hot, micron-size, rapidly moving spots on the cathode surface. The term “cathodic arc” is sometimes used in the literature since the plasma ions originate only from the cathode material. The formation of cathode spots is related to the

mechanism of electron emission. The anode, in contrast, collects electrons passively, i.e. it does not contribute to the plasma production as long as the current level is relatively low (that is, typically, less than 1 kA). The phenomenology and physics of cathode spots have recently been reviewed by Jüttner et al. [9]. It has been shown [10] that the current density and plasma density at these spots are extremely high $\sim 10^{12}$ A/m² and $\sim 10^{26}$ m⁻³, respectively. The cathode material suffers a complicated transition from the solid phase to an expanding, non-equilibrium plasma via liquid and dense, equilibrium non-ideal plasma phases [11]; thus vacuum arc plasma formation should not be confused with evaporation or sputtering. The pressure in a cathode spot is extremely high (up to 10^{10} Pa (10^5 bar), Ref. [12]) and the plasma rapidly expands into the vacuum ambient under the intense pressure gradient. Ions are accelerated by the combined forces of the pressure gradient, local electric fields and electron-ion friction [13,14]. The final ion velocity is $v_i = 1\text{--}2 \times 10^4$ m/s, nearly independent of their mass [15]. Ions are supersonic because the ion sound speed [16]:

$$v_s = \left(\frac{kT_e + \gamma kT_i}{m_i} \right)^{\frac{1}{2}} \approx 2 \left(\frac{kT}{m_i} \right)^{\frac{1}{2}} \quad (1)$$

is smaller than v_i (for example, $v_s \approx 4 \times 10^3$ m/s for a copper plasma with $T_e = T_i = T = 3$ eV). In Eq. (1), k is the Boltzmann constant, T is the temperature and m denotes the mass, with the indices “e” and “i” for electrons and ions, respectively. The ratio of specific heats, γ , is about 3. The fact that $v_s < v_i$ is an interesting feature that becomes important for the MePIID techniques.

Another interesting feature of vacuum arcs is that, in contrast to most gaseous plasmas, the metal plasma is fully ionized with a mean ion charge state mostly greater than 1+. Each cathode material has its own specific charge state distribution (CSD) which becomes constant for arc duration longer than 100 μ s. Ion CSDs of vacuum arcs have been measured by time-of-flight charge-to-mass spectrometry [17,18] and calculated for all conductive elements of the periodic table [19,20]. The element-specific CSDs can be enhanced (i.e. the mean ion charge states are increased) by applying an external magnetic field [21,22] or by using pulsed high currents [23].

An inherent feature of vacuum arc cathode spots is that not only plasma is formed from the cathode material but also liquid droplets (solid particles in the case of carbon) [24–27]. These droplets are of size 0.1–10 μ m and are often called “macroparticles” to emphasize their massive nature compared to plasma particles. Macroparticles are not acceptable for most applications, and “cleaning” methods are required. The most common method for separating plasma and macroparticles is to

use a curved magnetic filter (Fig. 1). Macroparticles move along almost straight trajectories due to their inertia while the plasma can be guided to a substrate location that is not line-of-sight to the cathode spot. Depending on the material and temperature, macroparticles either stick to the filter walls or “bounce off” in directions where they get caught by baffles. The plasma is guided when the electrons are magnetized, that is when the electron cyclotron radius:

$$r_e = \frac{m_e v_{\perp}}{eB} \approx \sqrt{8kT_e m_e / \pi} / eB \quad (2)$$

is much smaller than the minor duct radius and the collision frequency is smaller than the electron cyclotron frequency:

$$\omega_{pl,e}^{-1} = (\epsilon_0 m_e / e^2 n_e)^{1/2} \quad (3)$$

In these equations, e is the elementary charge, B is the magnetic field strength, v_{\perp} is the electron velocity perpendicular to the direction of the magnetic field, n_e is the electron density and ϵ_0 is the permittivity of vacuum. The magnetic field strength is usually not sufficient to magnetize ions but the ion motion is tied to the electron motion by plasma-internal electric fields and thus the plasma as a whole follows the magnetic field lines (model of “plasma optics”). A positive electric potential of the filter wall enhances the transport of ions. The mechanism of plasma transport is the subject of a number of papers (see, for instance, Refs. [28–34]. Aksenov and co-workers pioneered this field and introduced a 90° filter [28,35]. Storer et al. [32] found that the plasma transport efficiency decreases exponentially with the length of the filter (efficiency is defined as the ratio of the number of ions leaving the filter to the number entering it). A high filter efficiency of 25% can be obtained by using an optimized magnetic field strength (20–100 mT) and positive wall bias (~ 20 V) [29,36]. However, macroparticle removal is not perfect when using 45, 60 or even 90° curved ducts. Recently an S-shaped filter [37] was developed, which has an acceptable transport efficiency of 6% (like two 25% filters in series) with no detectable amounts of macroparticles (Fig. 2). Macroparticle filters can operate in dc or pulsed mode. Quarter-torus macroparticle filters have been down-scaled to a very small size (minor duct radius 5 mm, filtered ion current 1 A, Fig. 4 in Ref. [38]) as well as up-scaled to very large sizes and currents (minor radius 10 cm and filtered ion current 70 A, Ref. [39]).

3. Metal plasma immersion ion implantation and deposition (MePIID)

3.1. Implantation versus deposition

Metal vapors and plasmas have the feature of condensing on surfaces; the sticking coefficient is close to

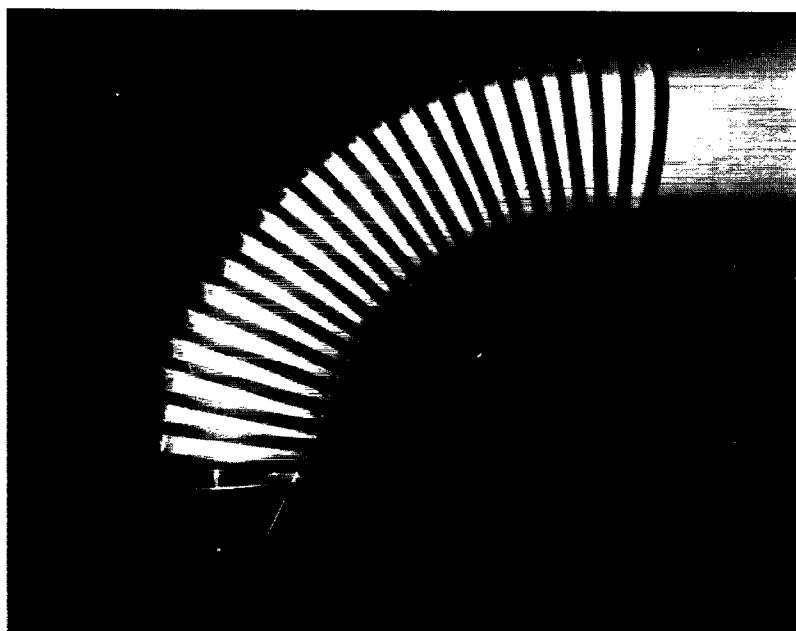


Fig. 1. Vacuum arc plasma streaming through a 90° macroparticle filter (quarter torus with major radius 15 cm, minor radius 3 cm; shown here is a “freestanding” filter allowing to observe the plasma flow (platinum); arc current = current through filter coil = 200 A).

one on surfaces that are colder than the temperature of the atoms and ions (which is usually the case). Therefore, in contrast to PIII with gaseous plasmas, PIII with a metal plasma is – in most configurations – a hybrid ion implantation and film deposition technique, and therefore a “D” for “deposition” is added to the acronym: MePIIID. The technique is made extremely versatile by choosing the ratio of deposition and implantation phases, ion energy and related projected implantation range, ion beam mixing of deposited film and substrate, etc. The details will be discussed below.

The possibilities of PIII are greatly extended when film formation is added to the ion implantation process.

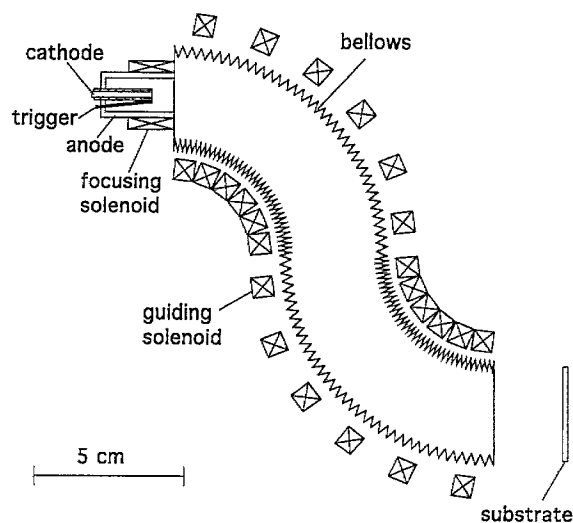


Fig. 2. S-shaped magnetic filter for the removal of macroparticle from cathodic arc plasmas, after [37].

First attempts were made by alternating PIII with sputter deposition [40]. In this work, stainless steel was alternately coated with Ti and implanted with nitrogen by PIII. A similar approach was tested for the formation of various niobium oxide phases (magnetron sputtering followed by oxygen PIII) [41]. In these cases, films were treated with PIII but no metal plasma was directly used to deposit them.

Brown et al. [42,43] proposed in the early 1990s a novel surface modification technique by combining PIII and cathodic arc deposition. They implanted yttrium ions into silicon wafers by pulse-biasing the substrate, and they formed also a titanium–yttrium multilayer structure with atomic mixing at chosen interfaces by using two (unfiltered) vacuum arc plasma sources. The vacuum arcs were pulsed, and each arc pulse was synchronized with a substrate bias pulse, Fig. 3a and b. Implantation and deposition phases are determined by the presence or absence of the high voltage substrate bias. Since the bias pulses (30 kV, 1 μs) were shorter than the arc pulses (2 μs), films were formed that were bonded to the substrate through an atomically mixed zone. The formation of an intermixed Ti/Si layer was also studied in a similar experiment in which a filtered cathodic arc was used [44].

In the above described experiments, each arc pulse was synchronized with a single bias pulse. The overall efficiency of MePIIID can be drastically increased by using long arc pulses (or even d.c. arc operation) with gated or cw pulse bias sequences [45], as indicated in Fig. 4a and b. The ratio of ion implantation and deposition is here tuned by the duty cycle of the bias voltage.

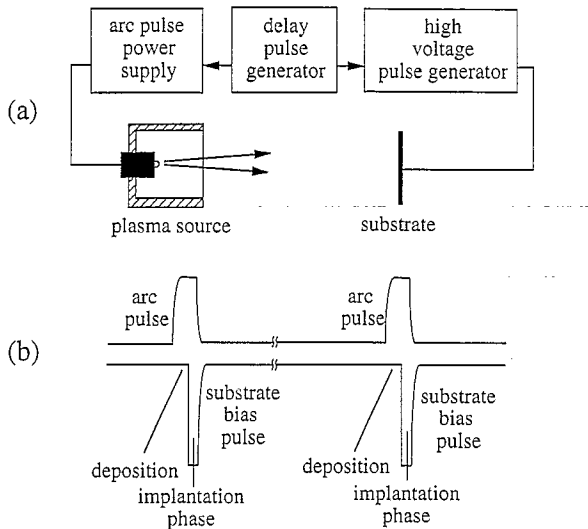


Fig. 3. (a) Schematic of the arrangement of the first MePIIID experiments; (b) sequences of arc and bias pulsing (after [42,43]).

Wood et al. [46] extended the bias pulses for the whole duration of the arc pulses, thus achieving pure ion implantation (without film deposition). They tested this concept by implanting erbium into various substrates at an applied voltage of 100 kV.

Sroda et al. [47] developed a filtered vacuum arc system and modified the previous approaches by replacing the pulsed substrate bias by a d.c.-bias, i.e. only the plasma production by the arc was pulsed (Fig. 5a and b). Since the filtered vacuum arc plasma flow is fully ionized, all particles (aluminum ions in this case) are accelerated in the sheath between plasma and substrate. In this way, plating-free aluminum ion implantation into silicon was obtained. This concept was later applied to dope p-type <100> Si with antimony [48].

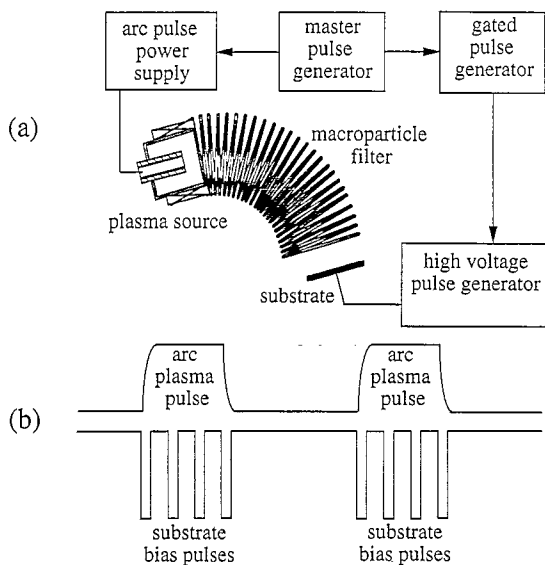


Fig. 4. (a) MePIIID with long arc pulses and gated bias pulses; (b) sequences of arc and bias pulsing (after [45]).

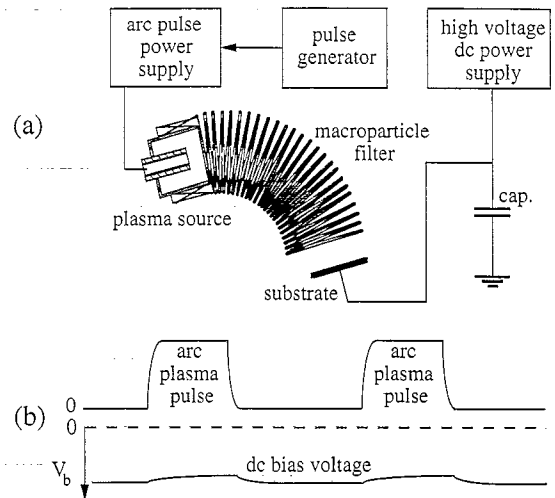


Fig. 5. (a) Arrangement for metal ion implantation without film deposition; (b) sequences of arc and bias pulsing (after [47]).

3.2. Ion implantation and sheath formation when using vacuum arc plasmas

In the following we focus on the MePIIID version when a sequence of bias pulses is applied to a conductive substrate. Other cases can be derived similarly. When a negative high voltage pulse is applied to the substrate immersed in a metal plasma, the physical processes are similar to those of “conventional” gaseous PIII (models of PIII are discussed, for instance, in Refs. [49–55]). Electrons are repelled from the substrate on a fast timescale, of the order of the inverse electron plasma frequency, see Eq. (3), and the so-called ion matrix sheath is formed. Ions are accelerated across the sheath on a slower timescale, of the order of the inverse ion plasma frequency,

$$\omega_{pi,i}^{-1} = \left(\epsilon_0 m_i / e \sum_{Z=1}^{Z_{\max}} Z^2 n_i^{Z+} \right)^{1/2} \quad (4)$$

where $Z=1, 2, \dots, Z_{\max}$ are the ion charge states present in the vacuum arc plasma and n_i^{Z+} are their respective densities. As the ions are accelerated, their density decreases, resulting in the space-charge limited flow. The initial ion matrix sheath expands (initially with the ion sound speed, Eq. (1)) until a steady-state sheath is formed. For instance, assuming a titanium plasma with a plasma density of 10^{17} m^{-3} the characteristic times are $2\pi/\omega_{pe} \approx 0.3 \text{ ns}$ and $2\pi/\omega_{pi,i} \approx 50 \text{ ns}$. Often, the bias pulses have slower rise and fall times, and the effect on the ion energy and dose must be taken into account [49].

Apart from the condensability, vacuum arc plasmas have some peculiarities, as discussed in Section 2:

- (1) multiply charged ions are present;
- (2) vacuum arc cathode spots are prolific producers of fully ionized plasma;

- (3) the plasma flow velocity is supersonic with respect to the ion sound speed.

These peculiarities lead to some interesting consequences.

Consequences of (i). The presence of several ion charge states gives rise to several ion energies,

$$E_i^{Z+} = |ZV_b| + E_0 \quad (5)$$

where E_0 is the ion energy corresponding to the flow velocity, $E_0 = m_i v_0^2/2$, and V_b is the applied negative bias voltage. Ions crossing the full sheath width acquire the energy given by Eq. (5). The ion energy becomes time dependent for finite rise and fall times of the bias voltage, $V_b(t)$. The various ion energies are related to various sputter rates. An effective sputter rate can be defined as:

$$\bar{\gamma} = \frac{\sum_{Z=1}^{Z_{\max}} \gamma_Z(E_i^Z) n_i^Z}{\sum_{Z=1}^{Z_{\max}} n_i^Z} \quad (6)$$

where $\gamma_Z(E_i^Z)$ is the energy-dependent sputter rate of Z -fold charged ions. The thickness of the initial ion matrix sheath is given by:

$$s_0 = \left(\frac{2\epsilon_0 |V_b|}{\bar{Z} e n_i} \right)^{1/2} \quad (7)$$

thus it is thinner than in “standard” PIII by a factor of $\bar{Z}^{-1/2}$, where \bar{Z} is the mean ion charge,

$$\bar{Z} = \frac{\sum_{Z=1}^{Z_{\max}} Z n_i^Z}{\sum_{Z=1}^{Z_{\max}} n_i^Z} \quad (8)$$

and n_i denotes the total ion density (all charge states) at the plasma-sheath boundary. Similarly, the ion plasma frequency (Eq. (4)) is enhanced by a factor \bar{Z} .

Consequences of (ii). The plasma density, $n = n_e = \bar{Z} n_i$, is relatively high and the inverse electron and ion plasma frequencies are usually shorter than the pulse rise and fall times. The ion fluxes and related ion currents and deposition rates are high compared with other implantation and deposition techniques.

Consequences of (iii). In the standard sheath model, introduced by Stewart and Lieberman [49], it is assumed that the ion current is derived from the number of ions uncovered by the expanding sheath. Later it was pointed out that ions enter the sheath with a non-zero velocity that allows a finite, stationary sheath to exist with non-zero ion current [50,56]. The ion velocity is due to acceleration in the presheath and equals the ion sound speed in the stationary case (Bohm criterion). Because the ions of a vacuum arc have already a supersonic speed, the equation for the sheath thickness reads:

$$j_i = \bar{Z} e n_i \left(\frac{ds}{dt} + v_i \right) \quad (9)$$

A simple estimate shows that the ion current at the

beginning of a high voltage pulse is dominated by the ds/dt term. In the absence of high voltage bias, ions arrive at the substrate with the flux $J_i = n_i v_i$ and their electrical current is compensated by the electron flux. Eq. (9) is true when the plasma flow is normal to the substrate area. For the side faces of a three-dimensional substrate, the ion flux becomes different in the deposition and implantation phases (ion saturation current and Child–Langmuir current, respectively):

$$j_i \approx \begin{cases} \bar{Z} e n_i (8kT_e/\pi m_i)^{1/2}/4 & \text{deposition phase} \\ 4\sqrt{2\bar{Z}e\epsilon_0}|V_b|^{3/2}/9\sqrt{m_i}s^2 & \text{implantation phase} \end{cases} \quad (10)$$

where s is the local sheath thickness. Another consequence of the supersonic velocity is that there are shock waves formed upstream of the substrate, and a wake downstream. A sheath thickness greater than the characteristic dimension of the substrate is required if ion implantation into a three-dimensional substrate with the flowing plasmas is performed (otherwise the wake side will have a very low dose). The large sheath thickness can be obtained by choosing a very small plasma density, combined with a high bias voltage. A relatively uniform implantation of aluminum ions into all faces of a $(2\text{ cm})^3$ cube was achieved in this way [47].

3.3. Ion deposition using vacuum arc plasmas

Substrate bias is very small or absent in the deposition phase of MePIIID. Metal ions arriving at the substrate surface form an adhesive film; the sticking coefficient is close to unity. Because the ions have a considerable energy, E_0 , even in the absence of a bias, see Eq. (5), they are energetic enough to overcome local potential barriers that hinder motion along the surface. They move on the surface sufficiently to be trapped at favorable sites. Metal films produced by filtered vacuum arc plasmas are therefore denser and smoother than those fabricated with other deposition methods such as sputtering or evaporation. Similar effects have been observed in ion beam assisted deposition (IBAD) of thin films [57].

The implantation and deposition phases are alternated in the MePIIID technique so as to bombard the freshly deposited film with energetic ions. Both direct and recoil implantation are therefore characteristic of MePIIID, leading to the formation of an intermixed layer, which is responsible for the superior adhesion of the films formed. It also reduces the stress associated with the structural mismatch of substrate and film material, in comparison with non-intermixed deposition. As the film grows, an increasing fraction of ions is implanted not only into the original substrate but also into the deposited film. To enhance the effect of intermixing but reduce sputtering of the deposited layer at a later stage, MePIIID can be started with a very high substrate bias

and, after an intermixed layer has been formed, continued with a relatively low bias. When the growing film is thicker than the implantation depth, ion implantation does not contribute anymore to intermixing but may be essential to the structure of the film.

For a number of applications, cathodic arc deposition can be performed without any ion accelerating substrate bias. Plasma deposition with vacuum arcs was already in use at the end of the last century for the replication of phonograms [58]. In the last decade, cathodic arc deposition has become an established technology for various coatings applications [59–61].

3.4. MePIIID in the presence of reactive gases

The MePIIID technique can be considerably extended by including a reactive gas such as nitrogen or oxygen. Metal ions collide with the gas molecules in transit from the vacuum arc plasma source to the substrate, and the gas becomes partially ionized. Metal and gas react preferentially on the substrate surface (because of the energy and momentum conservation), forming a compound film. If the pressure is increased so that the mean free path of the metal ions becomes comparable to the source–substrate distance, the kinetic ion energy, charge state and deposition rate decrease. Examples are given in Section 4.

MePIIID is a technique related to but different from other deposition techniques such as IBAD [62,63] and ion plating [64,65]. The idea of IBAD is to deposit a film on the substrate surface (e.g. by evaporation or sputtering) and to modify its structure with ions of moderate energy (often argon, 50–500 eV). In contrast to MePIIID, IBAD requires an external ion source. The principle of ion plating is similar but the ion bombardment is achieved by using gas ions accelerated in the cathode sheath of an abnormal glow discharge. A film is deposited only if the deposition rate from the evaporation source exceeds the sputter rate. Thus, in contrast to MePIIID, ion plating is always performed in an inert or reactive gas environment.

4. Some applications

4.1. General remarks

The range of applications is very broad due to the wide range of plasma species and energies. Therefore, only some applications are named with the focus on the results obtained by the Plasma Applications Group in Berkeley. Typically, we use repetitively pulsed, compact sources of magnetically filtered vacuum arc plasmas such as described in Ref. [66]. Typical discharge parameters were: arc current 100–250 A, arc pulse duration 0.5–5 ms, pulse repetition rate 1–10 pps. The plasma

density at the substrate location was 10^{16} – 10^{19} m⁻³ depending on cathode material, arc current and geometry. In most of our experiments, the substrate was biased using a high voltage pulse generator that is capable of delivering a maximum current of 10 A at a maximum voltage of –2.4 kV. The duration of each bias pulse was usually of 1–10 μ s, with a duty cycle up to 50% (compare Fig. 4). In some experiments, a thyatron pulse generator with a step-up transformer was used to apply pulses of up to –30 kV.

4.2. Metal films

Stainless steel suffers long-term corrosion in harsh environments. Using MePIIID, we have deposited palladium and tungsten on polished stainless steel samples. Adhesion was improved by applying high bias pulses (–2 kV) to form an intermixed layer. Corrosion tests showed improved behavior of the treated samples.

MePIIID was applied to metallize semiconductors at room temperature. We have deposited films of Pt, Au, Al, Cu, Ni and Ag, with thickness from 3 to 200 nm, on Si and GaAs substrates.

Adhesive films of Cu, Ag and Au have been deposited on Al samples (~ 100 cm²) to modify the radio frequency properties of cavities and waveguides. The aluminum samples were cleaned in situ by argon sputtering and the films were deposited using a pulsed bias of –2.0 kV. For comparison, deposition was also done on samples without biasing but otherwise identical conditions. The adhesion of the films made without bias appeared to be much worse, as easily shown by a simple “tape test” using Scotch Magic Tape no. 810. Improved adhesion is not attributed to heating because the substrates were kept at room temperature (the substrate holder was water-cooled). Instead, we believe that the combined effects of “ion cleaning” and “ion stitching” is responsible for the improved adhesion observed. In the energy range of about 2–6 keV (i.e. bias –2 kV), ion cleaning is efficient because the sputtering coefficient is large, and “ion stitching” or “mixing” occurs in a depth of the order of 10 nm [67].

Carbon–carbon (C–C) composite materials are used for structural applications due to their high mechanical strength and chemical stability at temperatures of up to 3000 K. Adhesion of metal films to the composite is a problem with sputtering and other “conventional” deposition techniques. The substrate in our experiment was made from carbon fibers impregnated in an epoxy resin matrix to form a two-dimensional mat. We used a two-step process to deposit a well-bonded nickel film [68]. In the first step, an intermixed layer was produced (pulse bias of –2.0 kV). The formation of this atomically intermixed layer was confirmed by Auger electron spectroscopy (AES). In the second step, a 1 μ m thick nickel film was deposited without substrate bias. The

adhesion of the film exceeded $6.8 \times 10^7 \text{ N/m}^2$ (9800 psi), which was the upper limit of the Sebastian Pull Tester used.

4.3. Compound films

Compound films have been deposited using MePIIID in the presence of reactive gases. For instance, a stoichiometric Al_2O_3 film of 200 nm thickness was deposited on steel [43]. An intermixed layer was obtained by applying a pulsed bias voltage of -30 kV , leading to an average ion energy of about 70 keV. The layer was found to be 100 nm thick (measured by Rutherford backscattering spectroscopy (RBS) and AES). Adhesive alumina films improve the wear resistance of steel.

Highly adherent films of alumina and chromia have been deposited on SiC and FeAl, starting with high bias (-2 kV) to form the intermixed layer, followed by lower bias (-200 V) for IBAD-like film deposition. The films had thicknesses in the range 0.2 to $1.5 \mu\text{m}$. They were investigated by RBS, X-ray diffraction and adhesion pull testing. They have been subject to temperature cycling between ambient and 1000°C , and adhesion was maintained. This work is ongoing.

An alloy cathode of $\text{Ag/YBa}_2\text{Cu}_3\text{O}_x$ was used to deposit a thin 100 nm film on silver and silicon substrates. The samples were annealed ex situ in an oxygen atmosphere to obtain the high oxygen content required for the superconducting properties. We also deposited $\text{Ag/YBa}_2\text{Cu}_3\text{O}_x$ on insulating Al_2O_3 films that were previously deposited on Ag and Si substrates by reactive MePIIID. Pulsed bias played here an important role for the reduction of stress: cracking followed by delamination of the films was completely avoided [45].

UHV-compatible, black surfaces of accelerator components have been obtained by depositing CuO using MePIIID with copper electrodes in an oxygen atmosphere of up to 30 Pa [69]. The parts were vacuum baked twice in a furnace at 150°C for 8 h, and the films remained highly adherent (pull strength exceeded 85 MPa).

High-temperature corrosion-resistant films of alumina-silica ("Mullite") have been formed using two filtered cathodic arc sources (one for Al, and one with a Si/Al alloy cathode) in an oxygen atmosphere [70]. This multiple-source approach was also used to deposit a multilayer structure of a:C (see Section 4.4.) and TiC on silicon [70].

4.4. Amorphous diamond films

Amorphous hard carbon films (a:C, also called amorphous diamond or hydrogen-free diamond-like carbon) have a high content of fourfold coordinated sp^3 carbon atoms (diamond bonds). These films are smooth, hard, transparent, insulating and have a low friction coefficient.

They are extensively studied due to their wide range of applications, see, for instance, the review by Robertson [71]. It has been shown that the hardest films can be deposited by cathodic arc deposition [72–78]. MePIIID with filtered carbon plasmas offers a convenient way to tailor the ion energy and related structure and properties of a:C films [79,80]. These films have been applied to reduce wear of magnetic Al_2O_3 -TiC and Ni-Zn ferrite recording heads [81,82]. The high compressive stress can be investigated by Raman spectroscopy and modified by the ion energy (bias) during film growth [83]. By varying the bias, an a:C multilayer structure (on Si) with interesting properties has been formed [84].

4.5. Increasing the retained dose

The retained dose of ions implanted into a substrate is always smaller than the incident dose (fluence) because some of the implanted ions are sputtered. This is a well-known effect, which becomes dominant when the fluence is of order $10^{17} \text{ ions/cm}^2$ or higher. Clapham et al. [85] proposed to deposit a protective "sacrificial" layer (such as carbon) prior to ion implantation. MePIIID offers an elegant way of depositing and renewing the sacrificial layer during ion implantation. The ion implantation can be part of the MePIIID process or performed with a separate ion accelerator. Monte Carlo simulations using the dynamic TRIM code (T-DYN, Ref. [86]) illustrate the substantial increases in the retained dose [67,87].

5. A new approach: pulsing both plasma and substrate potential, and increasing the ion charge state

Recently it has been shown that a pulsed metal plasma can be produced at elevated potential with a single grounded power supply and a modified Marx generator [88]. Another modification of the Marx generator is shown in Fig. 6. Here pulses of both polarity are obtained. The positive pulse is used to shift the plasma potential, and the negative pulse is used to bias the substrate. In doing so, a larger total difference between plasma potential and substrate potential is achieved. One advantage is that the voltage at the vacuum feed-throughs is smaller than the voltage across the sheath between plasma and substrate. Another focus of our research is to increase the ion charge state, which gives rise to higher ion energies, see Eq. (5).

A Marx generator is a simple voltage-multiplying scheme that was introduced decades ago [89]. The idea is to charge capacitors that are electrically in parallel and switch them in series; the total voltage is the charging voltage times the number of capacitors (losses neglected). The modified Marx generator, Fig. 6, works as follows: the capacitors are charged via a charging

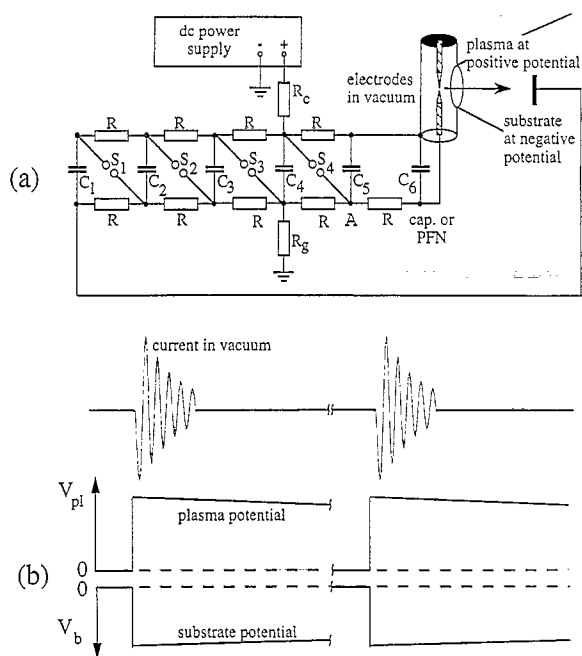


Fig. 6. (a) MePIII using a modified Marx generator; (b) sequences of discharge current, plasma potential and substrate bias pulses.

resistor until the gap between the electrodes in vacuum breaks down. The distance between these electrodes is small (about 1 mm or less) to make sure that this gap breaks down first. As a result, plasma is formed and the potential of point "A" (Fig. 6) is shifted negatively. This causes breakdown of the spark gap next to "A" (we used simple air gaps as switches), and all the other spark gaps of the Marx generator follow. The ground potential is placed at one of the stages in the middle so as to obtain a positive potential on one side (shifting the plasma potential positively) and a negative potential on the other side (used for substrate biasing). An additional "trick" to ensure synchronized breakdown of vacuum gap and Marx gaps is to build a pick-up coil around the main high-current discharge (not shown). The coil serves as a high voltage pulse transformer for triggering one of the Marx spark gaps. One advantage of the presented scheme is that the high discharge current, which is necessary to form highly ionized metal ions, does not flow through any of the Marx gaps in air (in contrast to a similar scheme described in Ref. [90]).

High ion charge states have been measured using a time-of-flight technique. For instance, charge states as high as $5+$ and $6+$ have been found for copper [91]. The schematic of Fig. 6 was developed with five stages and tested with a charging voltage of 10 kV. It represents a scheme for pure ion implantation since a high voltage sheath is always present when the plasma is produced. For a sheath voltage of about 50 kV and a mean ion charge state of $5+$ (copper), an ion energy of 250 keV is obtained although the charging voltage was only 10 kV. This concept opens up the possibility of doing

high energy ion immersion implantation at moderate charging voltages. High energy implantation experiments are in progress.

6. Conclusions

Metal plasma immersion ion implantation and deposition (MePIIID) is a versatile technique, representing a combination of cathodic arc deposition and plasma immersion ion implantation. Various approaches have been developed, ranging from low energy deposition to high energy ion implantation without film formation. The properties of macroparticle-filtered, fully ionized cathodic-arc metal plasmas allow one to modify surfaces and synthesize films uniquely and efficiently. This includes the formation of metal, compound and amorphous diamond films. New approaches include the use of improved macroparticle filters, the combination of several plasma sources and better pulsing techniques. It can be anticipated that, with the commercial availability of cathodic arc deposition facilities and PIII systems, MePIIID will find a number of applications such as the deposition of amorphous carbon for wear applications (magnetic recording heads, tools, etc.).

Acknowledgement

The paper contains results obtained in collaboration with many colleagues. In particular I would like to thank I. Brown, O. Monteiro, S. Anders, R. MacGill, M. Dickinson and Z. Wang. This work was supported by the US Department of Energy, Division of Advanced Energy Projects, under contract No. DE-AC03-76SF00098.

References

- [1] J.R. Conrad, J.L. Radtke, R.A. Dodd, F.J. Worzala, N.C. Tran, *J. Appl. Phys.* 62 (1987) 4591.
- [2] J.R. Conrad, Method and Apparatus for Plasma Source Ion Implantation, US Patent 4764394, 1988.
- [3] Papers from the First Int. Workshop on Plasma-Based Ion Implantation, *J. Vac. Sci. Technol. B* 12 (1994) 815.
- [4] Papers from the Second Int. Workshop on Plasma-Based Ion Implantation, *Surf. Coat. Technol.* 85 (1996) 1.
- [5] J.V. Mantese, I.G. Brown, N.W. Cheung, G.A. Collins, *MRS Bulletin* 21 (1996) 52.
- [6] K. Walter, R. Adler, personal communication during the 10th IBMM, Albuquerque, Sept., 1996.
- [7] J. Chen, J. Blanchard, J.R. Conrad, R.A. Dodd, *Surf. Coat. Technol.* 53 (1992) 267.
- [8] J. Chen, J.P. Blanchard, J.R. Conrad, P. Fetherston, X. Qiu, *Wear* 165 (1993) 97.
- [9] B. Jüttner, V.F. Puchkarev, E. Hantzschke, I. Beilis, Cathode Spots, in: R.L. Boxman, D.M. Sanders, P.J. Martin (Eds.), Hand-

- book of Vacuum Arc Science and Technology, Noyes, Park Ridge, New Jersey, 1995, 73–281.
- [10] A. Anders, S. Anders, B. Jüttner, W. Böttcher, H. Lück, G. Schröder, *IEEE Trans. Plasma Sci.* 20 (1992) 466.
 - [11] A. Anders, S. Anders, Förster A., I.G. Brown, *Plasma Sources Sci. Technol.* 1 (1992) 263.
 - [12] G.A. Mesyats, D.I. Proskurovsky, *Pulsed Electrical Discharge in Vacuum*, Springer-Verlag, Berlin, 1989.
 - [13] E. Hantzsch, *J. Phys. D: Appl. Phys.* 24 (1991) 1339.
 - [14] E. Hantzsch, *IEEE Trans. Plasma Sci.* 34 (1992) 34.
 - [15] J. Kutzner, H.C. Miller, *J. Phys. D: Appl. Phys.* 25 (1992) 686.
 - [16] F.F. Chen, *Plasma Physics and Controlled Fusion*, Plenum Press, New York, 1984.
 - [17] I.G. Brown, X. Godechot, *IEEE Trans. Plasma Sci.*, PS-19 (1991) 713.
 - [18] I.G. Brown, *Rev. Sci. Instrum.* 65 (1994) 3061.
 - [19] A. Anders, *The Periodic Table of Vacuum Arc Charge State Distributions*, Lawrence Berkeley National Laboratory, Berkeley, preprint LBL-38672, May 1996.
 - [20] A. Anders, *Phys. Rev. E* 55 (1997) 696.
 - [21] E. Oks, I.G. Brown, M.R. Dickinson, R.A. MacGill, P. Spädtke, H. Emig, B.H. Wolf, *Appl. Phys. Lett.* 67 (1995) 200.
 - [22] E.M. Oks, A. Anders, I.G. Brown, M.R. Dickinson, R.A. MacGill, *IEEE Trans. Plasma Sci.* 24 (1996) 1174.
 - [23] A. Anders, I. Brown, M. Dickinson, R. MacGill, *Rev. Sci. Instrum.* 67 (1996) 1202.
 - [24] J.E. Daalder, *J. Phys. D: Appl. Phys.* 9 (1976) 2379.
 - [25] D.T. Tuma, C.L. Chen, D.K. Davis, *J. Appl. Phys.* 49 (1978) 3821.
 - [26] S. Anders, A. Anders, K.M. Yu, X.Y. Yao, I.G. Brown, *IEEE Trans. Plasma Sci.* 21 (1993) 440.
 - [27] R.L. Boxman, S. Goldsmith, *Surf. Coat. Technol.* 52 (1992) 39.
 - [28] I.I. Aksenov, V.A. Belous, V.G. Padalka, V.M. Khoroshikh, *Sov. J. Plasma Phys.* 4 (1978) 425; *Russ. original: Fiz. Plazmy* 4 (1978) 758.
 - [29] A. Anders, S. Anders, I.G. Brown, *J. Appl. Phys.* 75 (1994) 4900.
 - [30] D.B. Boercker, D.M. Sanders, J. Storer, S. Falabella, *J. Appl. Phys.* 69 (1991) 115.
 - [31] C.A. Davis, I.J. Donnelly, *J. Appl. Phys.* 72 (1992) 1740.
 - [32] J. Storer, J.E. Galvin, I.G. Brown, *J. Appl. Phys.* 66 (1989) 5245.
 - [33] V.S. Veerasamy, G.A.J. Amaratunga, W.I. Milne, *IEEE Trans. Plasma Sci.* 21 (1993) 322.
 - [34] M.M.M. Bilek, D.R. McKenzie, Y. Yin, M.U. Chhowalla, W.I. Milne, *IEEE Trans. Plasma Sci.* 24 (1996) 1291.
 - [35] I.I. Aksenov, V.A. Belous, V.G. Padalka, *Instrum. Exp. Technol.* 21 (1978) 1416. *Russ. original: Priboory Tekh. Eksp.*, no. 5 (1977) 236.
 - [36] A. Anders, S. Anders, I.G. Brown, *Plasma Sources Sci. Technol.* 4 (1995) 1.
 - [37] S. Anders, A. Anders, M.R. Dickinson, R.A. MacGill, I.G. Brown, *Proc. of XVIIth Int. Symp. Disch. El. Insul. Vacuum*, Berkeley, CA, 1996, pp. 904–908.
 - [38] A. Anders, S. Anders, I.G. Brown, R.A. MacGill, M.R. Dickinson, *SPIE Proc. Series* 2259 (1994) 195.
 - [39] T. Schülke, A. Anders, P. Siemroth, *Proc. of XVIIth Int. Symp. Disch. El. Insul. Vacuum*, Berkeley, CA, 1996, pp. 914–917.
 - [40] J.R. Conrad, R.A. Dodd, S. Han, M. Madapura, J. Scheuer, K. Sridharan, F.J. Worzala, *J. Vac. Sci. Technol. A* 8 (1990) 3146.
 - [41] W. Ensinger, B. Rauschenbach, B. Stritzker, *Proc. of 2nd Int. Workshop on Plasma-Based Ion Implantation*, Sydney, Australia, 1995, unpublished.
 - [42] I.G. Brown, X. Godechot, K.M. Yu, *Appl. Phys. Lett.* 58 (1991) 1392.
 - [43] I.G. Brown, A. Anders, S. Anders, M.R. Dickinson, I.C. Ivanov, R.A. MacGill, X.Y. Yao, K.-M. Yu, *Nucl. Instrum. Methods Phys. Res. B* 8081 (1993) 1281.
 - [44] D.R. McKenzie, Y. Yin, E. Gerstner, M.M.M. Bilek, *Proc. of XVIIth Int. Symp. Disch. El. Insul. Vacuum*, Berkeley, CA, 1996, pp. 839–847.
 - [45] A. Anders, S. Anders, I.G. Brown, M.R. Dickinson, R.A. MacGill, *J. Vac. Sci. Technol. B* 12 (1994) 815.
 - [46] B.P. Wood, W.A. Reass, I. Henins, *Surf. Coat. Technol.* 85 (1996) 70.
 - [47] T. Sroda, S. Meassick, C. Chan, *Appl. Phys. Lett.* 60 (1992) 1076.
 - [48] Z. Xia, C. Chan, S. Meassick, R. Purser, *J. Vac. Sci. Technol. B* 13 (1995) 1999.
 - [49] R.A. Stewart, M.A. Lieberman, *J. Appl. Phys.* 70 (1991) 3481.
 - [50] G.A. Collins, J. Tendys, *Plasma Sources Sci. Technol.* 3 (1994) 10.
 - [51] J.R. Conrad, *J. Appl. Phys.* 62 (1987) 777.
 - [52] J.T. Scheuer, M. Schamim, J.R. Conrad, *J. Appl. Phys.* 67 (1990) 1241.
 - [53] B.P. Wood, *J. Appl. Phys.* 73 (1993) 4770.
 - [54] S. Qin, C. Chan, *J. Appl. Phys.* 79 (1996) 3432.
 - [55] S. Qin, Z. Jin, C. Chan, *J. Appl. Phys.* 78 (1995) 55.
 - [56] W. En, N.W. Cheung, *J. Vac. Sci. Technol. B* 12 (1994) 833.
 - [57] W. Ensinger, *Proc. of 10th Int. Conf. Ion Beam Modification of Materials*, Albuquerque, NM, 1996, unpublished.
 - [58] T.A. Edison, "Process of Duplicating Phonograms," U.S. Patent 484 582, 1892.
 - [59] R.L. Boxman, S. Goldsmith, *IEEE Trans. Plasma Sci.* 17 (1989) 705.
 - [60] R.L. Boxman, D.M. Sanders, P.J. Martin, *Handbook of Vacuum Arc Science and Technology*, Noyes Publications, Park Ridge, 1995.
 - [61] D.M. Sanders, D.B. Boercker, S. Falabella, *IEEE Trans. Plasma Sci.* 18 (1990) 883.
 - [62] G.K. Wolf, *J. Vac. Sci. Technol. A* 10 (1992) 1757.
 - [63] J.J. Cuomo, S.M. Rossnagel, H.R. Kaufman (eds.), *Handbook of Ion Beam Processing Technology*, Noyes, Park Ridge, 1989.
 - [64] P.A. Dearnley, *Proc. of Conf. on Ion Plating and Implantation*, Atlanta, GA, 1985, pp. 31–38.
 - [65] N.A.G. Ahmed, *Ion Plating Technology*, John Wiley, Chichester, 1987.
 - [66] S. Anders, A. Anders, I. Brown, *J. Appl. Phys.* 74 (1993) 4239.
 - [67] A. Anders, S. Anders, I.G. Brown, K.M. Yu, *Nucl. Instrum. Meth. Phys. Res. B* 102 (1995) 132.
 - [68] A. Anders, S. Anders, I.G. Brown, P. Chow, *Mat. Res. Soc. Symp. Proc.* 314 (1993) 205.
 - [69] R.A. MacGill, S. Anders, A. Anders, R.A. Castro, M.R. Dickinson, K.M. Yu, I.G. Brown, *Surf. Coat. Technol.* 78 (1996) 168.
 - [70] O.R. Monteiro, Z. Wang, I.G. Brown, *Proc. Xth Int. Conf. Ion Beam Modification of Materials*, Albuquerque, NM, 1996.
 - [71] J. Robertson, *Prog. Solid State Chem.* 21 (1991) 199.
 - [72] I.I. Aksenov, V.E. Strel'nitskij, *Surf. Coat. Technol.* 47 (1991) 98.
 - [73] I.I. Aksenov, S.I. Vakula, V.G. Padalka, V.E. Strel'nitskij, V.M. Khoroshikh, *Sov. Phys. Techn. Phys.* 25 (1980) 1164. *Russ. original: Zh. Tekh. Fiz.* 50 (1980) 2000.
 - [74] B.F. Coll, P. Sathrum, R. Aharonov, M.A. Tamor, *Thin Solid Films* 209 (1992) 165.
 - [75] J.J. Cuomo, D.L. Pappas, J. Bruley, J.P. Doyle, K.K. Saenger, *J. Appl. Phys.* 70 (1991) 1706.
 - [76] R. Lossy, D.L. Pappas, R.A. Roy, J.J. Cuomo, V.H. Sura, *Appl. Phys. Lett.* 61 (1992) 171.
 - [77] E.G. Gerstner, D.R. McKenzie, M.K. Puchert, P.Y. Timbell, J. Zou, *J. Vac. Sci. Technol. A* 13 (1995) 406.
 - [78] D.R. McKenzie, *Diamond. Relat. Mater.* 1 (1991) 51.
 - [79] S. Anders, A. Anders, I.G. Brown, B. Wei, K. Komvopoulos, J.W. Ager, K.M. Yu, *Surf. Coat. Technol.* 6869 (1994) 388.
 - [80] S. Anders, A. Anders, C.S. Bhatia, S. Raoux, D. Schneider, J.W. Ager, I.G. Brown, *Proc. 3rd Conf. on Appl. of Diamond Films and Related Materials*, Gaithersburg, MD, 1995, pp. 809–812.
 - [81] K. Komvopoulos, B. Wei, S. Anders, A. Anders, I.G. Brown, C.S. Bhatia, *J. Appl. Phys.* 76 (1994) 1656.

- [82] B. Bhushan, B.K. Gupta, R. Sundaram, S. Dey, S. Anders, A. Anders, I.G. Brown, *IEEE Trans. Magn.* 31 (1995) 2976.
- [83] J.W. Ager, S. Anders, A. Anders, I.G. Brown, *Appl. Phys. Lett.* 66 (1995) 3444.
- [84] S. Anders, A. Anders, J.W. Ager III, Z. Wang, G.M. Pharr, T.Y. Tsui, I.G. Brown, C.S. Bhatia, *Mat. Res. Soc. Proc.* 383 (1995) 453.
- [85] L. Clapham, J.L. Whitton, M.C. Ridgway, N. Hauser, M. Pertravic, *J. Appl. Phys.* 72 (1992) 4014.
- [86] J.P. Biersack, *Nucl. Instrum. Meth. Phys. Res. B* 5960 (1991) 21.
- [87] A. Anders, S. Anders, I.G. Brown, K.M. Yu, In-situ Deposition of Sacrificial Layers During Ion Implantation: Concept and Simulation, in: J.S. Williams, R.G. Elliman, M.C. Ridgway (Eds.), *Ion Beam Modification of Materials*, Elsevier, Amsterdam, 1996, pp. 1089–1092.
- [88] A. Anders, I.G. Brown, R.A. MacGill, M.R. Dickinson, *Proc. of XVIIth Int. Symp. Disch. El. Insul. Vacuum*, Berkeley, CA, 1996, pp. 625–629.
- [89] E. Marx, *Elektrotechnische Zeitschrift* 45 (1924) 652.
- [90] A.M. Tolopa, *Rev. Sci. Instrum.* 65 (1994) 3134.
- [91] A. Anders, I.G. Brown, R.A. MacGill, M.D. Dickinson, *Proc. of XVIIth Int. Symp. on Disch. and El. Insul. in Vacuum*, Berkeley, CA, 1996, pp. 625–629.